Analysis of Transients in Nonuniform and Uniform Multiconductor Transmission Lines

OLGIERD A. PALUSINSKI, SENIOR MEMBER, IEEE, AND ANYU LEE

Abstract —**Delay times of digital logic circuits are now becoming smaller than those of interconnections used in packaging. At high speeds, such interconnections no longer behave as simple short circuits, but take on the appearance of transmission lines. One may choose to solve the problem of delay by increasing the density of the system. This, however, introduces the problem of "cross talk." The analysis of delay and cross talk in a system of transmission lines is rather complex; for this reason, it is usually done with the aid of computer simulation. The present paper introduces a very efficient and flexible time-domain analysis technique to predict the reflections and cross talk. Numerical results show that this technique is indeed efficient and accurate in the transient analysis of general multiple coupled line systems. Furthermore, this algorithm will eventually be coded in a form of subroutine compatible with any standard CAD program, such as SPICE.**

I. Introduction

The TRANSIENTS in high-speed digital integrated circuits are characterized by a signal rise time shorter than one nanosecond. The interconnections in systems composed of such circuits have to be treated as multiple coupled transmission lines. A designer of interconnections must take into account effects associated with transmission lines such as delays, reflections and cross talk.

A possible solution to the problem of reflections is to decrease the length of the interconnections by increasing the system density. The trend toward greater density, however, brings about another problem, that of cross talk between the various conductors of the system. This coupling, which often exists between two adjacent transmission lines, may be strong enough for signals to appear on both lines when they are desired only on one. The problem of cross talk is present even if lines are terminated, and since these lines are carrying digital information, this unwanted coupling introduces false information into the system. The general category of extraneous voltages and currents due to reflections and cross talk is commonly called interconnection noise. Hence, in designing a high-speed digital system, both the circuits and the interconnections must be considered or system performance may be impaired. The analysis of system interconnections is involved owing to the presence of multiple lines and discontinuities caused by the abrupt changes of geometry at pads, pins, and even conductor bends. Such discontinuities are modeled by equivalent circuits which give satisfactory results for the transients of interest caused by the signals with rise times not smaller than 100 ps. Metal lines between the discontinuities are modeled as transmission lines. The lines on boards are treated as uniform. The lines on chip carriers, between chip pads and pins, are usually nonuniform owing to geometrical constraints. Thus when analyzing the signal transmission through the interconnections between the fast integrated circuit chips, one needs to deal with a model composed of various transmission lines interconnected through equivalent circuits representing the discontinuities.

A considerable amount of work has been done on the properties and applications of multiple coupled interconnections since 1970 and even earlier [1]–[8]. Almost all of them dealt with lossless lines, for which analysis can be greatly simplified after introducing the so-called normal propagation modes. The disadvantage of this mode-based analysis is mainly its inflexibility; for example, it cannot easily handle lossy and nonuniform coupled lines. Besides, this method is not efficient when lines are terminated with nonlinear networks, which is the case in practice. The lossy, uniform lines are computed using modal analysis in the frequency domain [6]–[8] and tedious, error-prone transforming procedures are necessary to obtain the results in the time domain. The modal analyses (in both the time and the frequency domain) are not applicable to nonuniform lines. A method based on perturbational techniques for analysis of a pair of nonuniform lines is presented in [9]. This approach involves complex procedures employing many simplifying assumptions, and its applicability is basically limited to two lines only. The computation of transmission line parameters has received much attention in the literature [10]–[12]. Such parameters are usually arranged in the form of conductance, resistance, inductance, and capacitance matrices and it is assumed here that those matrices are available.

The purpose of this paper is to present an effective method for computation of the transient response of multiple nonuniform transmission lines. The important feature

Manuscript received December 24, 1987; revised July 13, 1988. This work was supported by the IBM Corporation under Project F246U and by Prime Computer, Inc., under Contract RD248483. Experience gained by the authors while developing spectral techniques for circuit analysis under SRC Contract 83-01-038 was very helpful. Applications to electronic packaging engineering evolved in the work sponsored by SRC Contract 87-MP-086.

The authors are with the Department of Electrical and Computer Engineering and Computer Engineering, University of Arizona, Tucson, AZ 85721.

IEEE Log Number 8824266.

0018-9480/89/0100-0127$01.00

of the method is its flexibility in application to many types of transmission lines (lossless, lossy, uniform, nonuniform) and to arbitrary circuit terminations. Based on the final formula derived in this analysis, we can easily convert the transmission lines to general active resistive networks. Thus the time-domain transient behavior of coupled lines with terminating networks can be analyzed by general circuit simulation procedures.

The method derived in this paper is based on the spectral method often used in applications to the numerical solution of partial differential equations [13]–[15]. The essential idea is to approximate spatial or time derivatives by constructing a global interpolant through discrete data points. The most useful interpolants are Chebyshev and Legendre polynomials [16]. The advantage of spectral methods is that they are more accurate than finite difference or finite element methods, so that fewer grid points are needed. The stability theory for algorithms based on spectral techniques is not yet as developed as in the case of finite differences [17], but recent mathematical publications [14], [18] indicate efforts aimed at improving this situation.

In this paper we choose Chebyshev polynomials as the interpolants, because they have much simpler representation of derivatives and are very efficient in the computations owing to the relation with the fast Fourier transform (FFT).

II. Mathematical Model of Nonuniform Interconnection

A nonuniform interconnection is characterized as a transmission line with spatial variations of resistance, capacitance, etc., caused by changes in geometry or materials along the connecting direction. Under the TEM assumption we obtain a set of partial differential equations

$$\frac{\partial v}{\partial x} = -r(x)i - l(x)\frac{\partial i}{\partial t} \tag{1}$$

$$\frac{\partial i}{\partial x} = -g(x)v - c(x)\frac{\partial v}{\partial t} \tag{2}$$

where

$$v = v(x,t)$$

$$i = i(x,t).$$

We assume that equations are in dimensionless form; the scaled spatial variable is in the range $[-1,1]$.

The voltage v and current i must satisfy the boundary conditions:

$$v(-1,t) = \mathscr{F}[i(-1,t),t] \tag{3}$$

$$v(1,t) = \mathscr{G}[i(1,t),t]. \tag{4}$$

The symbols $\mathscr{F}$ and $\mathscr{G}$ represent operators which might be time varying and in general describe the ordinary differential equations characterizing the terminating networks.

The line voltage and current must also satisfy the initial conditions:

$$v(x,0) = h_1(x) \tag{5}$$

$$i(x,0) = h_2(x) \tag{6}$$

where $h_1(x)$ represents the initial voltage distribution and $h_2(x)$ is a function describing the initial current distribution. The functions $r(x), l(x), g(x), c(x)$ are determined from the electromagnetic field calculations and are assumed to be given.

For multiple coupled lines, we can generalize (1) and (2) to get

$$\frac{\partial v_j}{\partial x} = -\sum_{k=1}^{\mathscr{K}} r_{jk}(x)i_k - \sum_{k=1}^{\mathscr{K}} l_{jk}(x)\frac{\partial i_k}{\partial t} \tag{7}$$

$$\frac{\partial i_j}{\partial x} = -\sum_{k=1}^{\mathscr{K}} g_{jk}(x)v_k - \sum_{k=1}^{\mathscr{K}} c_{jk}(x)\frac{\partial v_k}{\partial t}$$

$$\text{for } j=1,2,3,\cdots,\mathscr{K} \tag{8}$$

where $\mathscr{K}$ denotes a number of lines (excluding the reference line):

$$v_j = v_j(x,t), \qquad j=1,2,\cdots,\mathscr{K}$$

$$i_j = i_j(x,t), \qquad j=1,2,\cdots,\mathscr{K}.$$

The functions of $r_{jk}(x), g_{jk}(x), l_{jk}(x)$, and $c_{jk}(x)$ are assumed to be given. The line voltages v_j and currents i_j must satisfy the boundary conditions:

$$v_j(-1,t) = \mathscr{F}_j[i_1(-1,t), i_2(-1,t),\cdots, i_{\mathscr{K}}(-1,t),t] \tag{9}$$

$$v_j(1,t) = \mathscr{G}_j[i_1(1,t), i_2(1,t),\cdots, i_{\mathscr{K}}(1,t),t] \tag{10}$$

where the symbols $\mathscr{F}_j$ and $\mathscr{G}_j$ are the operators representing the differential equations which describe the terminating networks.

The line voltages and currents at the moment $t=0$ (initial moment of transient analysis) are given in the form

$$v_j(x,0) = h_{1j}(x) \tag{11}$$

$$i_j(x,0) = h_{2j}(x) \tag{12}$$

where $h_{1j}(x)$ represents the initial distribution of voltages, and $h_{2j}(x)$ are functions describing initial distribution of line currents.

Introducing the vector notations

$$\boldsymbol{v} = [v_1, v_2, \cdots, v_{\mathscr{K}}]^T$$

$$\boldsymbol{i} = [i_1, i_2, \cdots, i_{\mathscr{K}}]^T \tag{13}$$

$$\boldsymbol{C}(x) = \{c_{jk}(x)\} \qquad \boldsymbol{L}(x) = \{l_{jk}(x)\}$$

$$\boldsymbol{R}(x) = \{r_{jk}(x)\} \qquad \boldsymbol{G}(x) = \{g_{jk}(x)\}$$

$$j,k = 1,2,\cdots,\mathscr{K}$$

we can write (7) and (8) in a convenient, compact form:

$$\frac{\partial \boldsymbol{v}}{\partial x} = -\boldsymbol{R}(x)\boldsymbol{i} - \boldsymbol{L}(x)\frac{\partial \boldsymbol{i}}{\partial t}$$
$$\frac{\partial \boldsymbol{i}}{\partial x} = -\boldsymbol{G}(x)\boldsymbol{v} - \boldsymbol{C}(x)\frac{\partial \boldsymbol{v}}{\partial t}. \quad (14)$$

The boundary conditions are written in the form

$$\boldsymbol{v}(-1,t) = \mathscr{F}[\boldsymbol{i}(-1,t),t] \quad (15)$$
$$\boldsymbol{v}(1,t) = \mathscr{G}[\boldsymbol{i}(1,t),t] \quad (16)$$

where $\mathscr{F}$ is a vector operator with the entries $\mathscr{F}_j(\cdot)$, $j = 1,2,\cdots,\mathscr{K}$, and $\mathscr{G}$ represents a vector with the entries $\mathscr{G}_j(\cdot)$, $j = 1,2,\cdots,\mathscr{K}$.

The initial conditions written in the vectorized form are

$$\boldsymbol{v}(x,0) = \boldsymbol{h}_1(x) \quad (17)$$
$$\boldsymbol{i}(x,0) = \boldsymbol{h}_2(x) \quad (18)$$

where

$$\boldsymbol{h}_1^T(x) = [h_{11}(x), h_{12}(x), \cdots, h_{1\mathscr{K}}(x)]$$
$$\boldsymbol{h}_2^T(x) = [h_{21}(x), h_{22}(x), \cdots, h_{2\mathscr{K}}(x)].$$

III. Formulation of Spectral Equations

In this part, we describe the approach for solving the interconnection line problem using the Chebyshev polynomials. At first, we need to decide how to expand the unknown variables in the Chebyshev series. We have following choices:

1) time-expansion approach
2) spatial-expansion approach.

Here we would like to concentrate on the second approach, because it gives a more convenient representation of boundary conditions and the derivations are simpler. The time-domain expansion method will be discussed in a separate report. In order to make the derivation of the algorithm easy to understand, we start with the single-line case and then extend the results to the multiline case.

Using Chebyshev polynomials to represent the variation in space, we can express the i and v as follows:

$$v = \sum_{n=0}^{\infty}{}' a_n(t)T_n(x) \quad (19)$$
$$i = \sum_{n=0}^{\infty}{}' b_n(t)T_n(x). \quad (20)$$

It is also convenient to assume here the expansion of derivatives in the form

$$\frac{\partial v}{\partial x} = \sum_{k=0}^{\infty}{}' a_k^*(t)T_k(x) \quad (21a)$$
$$\frac{\partial i}{\partial x} = \sum_{k=0}^{\infty}{}' b_k^*(t)T_k(x). \quad (21b)$$

The symbols $T_n(x)$ are Chebyshev polynomials and $a_n(t), b_n(t)$ are the coefficients of expansion to be determined. The expansion coefficients for the derivatives, $a_n^*(t), b_n^*(t)$, will later be replaced by simple combinations of $a(t)$ and $b(t)$. The symbol Σ' denotes the summation with the first component divided by 2. This notation simplifies the formulas and is commonly used in spectral techniques [19].

Inserting the expansions (19)–(21) into the model equations (1) and (2) yields

$$\sum_{k=0}^{\infty}{}' a_k^*(t)T_k(x) = -r(x)\sum_{k=0}^{\infty}{}' b_k(t)T_k(x) - l(x)\sum_{k=0}^{\infty}{}' \frac{db_k(t)}{dt}T_k(x) \quad (22a)$$
$$\sum_{k=0}^{\infty}{}' b_k^*(t)T_k(x) = -g(x)\sum_{k=0}^{\infty}{}' a_k(t)T_k(x) - c(x)\sum_{k=0}^{\infty}{}' \frac{da_k(t)}{dt}T_k(x). \quad (22b)$$

The line parameters, which are functions of x, are expanded in Chebyshev series:

$$r(x) = \sum_{k=0}^{\infty}{}' r_k T_k(x) \quad (23a)$$
$$l(x) = \sum_{k=0}^{\infty}{}' l_k T_k(x) \quad (23b)$$
$$g(x) = \sum_{k=0}^{\infty}{}' g_k T_k(x) \quad (23c)$$
$$c(x) = \sum_{k=0}^{\infty}{}' c_k T_k(x). \quad (23d)$$

The symbols r_k, l_k, g_k, and c_k represents constants defined as

$$r_k = \frac{\langle r(x), T_k(x)\rangle}{\langle T_k(x), T_k(x)\rangle}$$
$$g_k = \frac{\langle g(x), T_k(x)\rangle}{\langle T_k(x), T_k(x)\rangle}$$
$$l_k = \frac{\langle l(x), T_k(x)\rangle}{\langle T_k(x), T_k(x)\rangle}$$
$$c_k = \frac{\langle c(x), T_k(x)\rangle}{\langle T_k(x), T_k(x)\rangle}$$

where $\langle a, b\rangle$ denotes the inner product of a, b defined for Chebyshev polynomials [19]. Inserting (23) into (22), we get

$$\sum_{k=0}^{\infty}{}' a_k^*(t)T_k(x) = -\sum_{k=0}^{\infty}{}'\sum_{j=0}^{\infty}{}' r_j b_k(t)T_k(x)T_j(x) - \sum_{k=0}^{\infty}{}'\sum_{j=0}^{\infty}{}' l_j \frac{db_k(t)}{dt}T_k(x)T_j(x) \quad (24a)$$
$$\sum_{k=0}^{\infty}{}' b_k^*(t)T_k(x) = -\sum_{k=0}^{\infty}{}'\sum_{j=0}^{\infty}{}' g_j a_k(t)T_k(x)T_j(x) - \sum_{k=0}^{\infty}{}'\sum_{j=0}^{\infty}{}' c_j \frac{da_k(t)}{dt}T_k(x)T_j(x). \quad (24b)$$

Equations (24a) and (24b) have identical structures; therefore we shall continue the discussion of (24a) only. The same approach will then apply to (24b).

Performing the inner product of both sides of (24a) with $T_m(x)$, we get

$$\sum_{k=0}^{\infty}{}' a_k^*(t)\langle T_k(x), T_m(x)\rangle = -\sum_{k=0}^{\infty}{}'\sum_{j=0}^{\infty}{}' b_k(t) r_j \langle T_k(x)T_j(x), T_m(x)\rangle - \sum_{k=0}^{\infty}{}'\sum_{j=0}^{\infty}{}' l_j \frac{db_k(t)}{dt}\langle T_k(x)T_j(x), T_m(x)\rangle. \quad (25)$$

Considering the relations [19]

$$T_kT_j = \frac{1}{2}\left(T_{k+j} + T_{|k-j|}\right), \qquad k, j = 0,1,2,\cdots$$

$$\langle T_k, T_m\rangle = \delta_{km}$$

and using the vector notation, we write (25) in the form

$$\hat{A}^* = \hat{K}_r \hat{B} + \hat{K}_l \frac{d\hat{B}}{dt} \quad (26)$$

where

$$\hat{A}^* = \left[a_0^*(t), a_1^*(t), \cdots\right]^T$$

$$\hat{B} = \left[b_0(t), b_1(t), \cdots\right]^T$$

$$\hat{K}_r(i,j) = -\frac{1}{2}\left(r_{i+j} + r_{|i-j|}\right)$$

$$\hat{K}_l(i,j) = -\frac{1}{2}\left(l_{i+j} + l_{|i-j|}\right), \qquad i, j = 0,1,2,\cdots.$$

We shall now eliminate $a_k^*(t)$ by $a_k(t)$ using the relation [14]

$$a_n(t) = \frac{1}{2n}\left(a_{n-1}^*(t) - a_{n+1}^*(t)\right) \qquad \text{for } n = 1,2,\cdots. \quad (27)$$

$$Q = \begin{pmatrix} 0 & 1 & 0 & 0 & \cdots & 0 \\ 0 & 0 & 1 & 0 & \cdots & 0 \\ \vdots & \vdots & \vdots & \vdots & \ddots & \vdots \\ \frac{1}{2}(-1)^N & -(-1)^N & (-1)^N & -(-1)^N & \cdots & 1 \end{pmatrix} \quad (31b)$$

Truncating the series at $n = N$, we get

$$a_N(t) = \frac{1}{2N} a_{N-1}^*(t)$$

$$a_{N+1}(t) = \frac{1}{2(N+1)} a_N^*(t). \quad (28)$$

Writing the relations (27) and (28) in matrix form, with the truncation, we obtain

$$a^1 = HA^* \quad (29)$$

where

$$a^1 = \left[a_1(t), a_2(t), \cdots, a_{N+1}(t)\right]^T$$

$$A^* = \left[a_0^*(t), a_1^*(t), \cdots, a_N^*(t)\right]^T$$

and the $(N+1)\times(N+1)$ square matrix, H, has entries defined as follows:

$$h_{ij} = \begin{cases} \frac{1}{2i}, & 1 \leqslant i = j \leqslant N-1 \\ -\frac{1}{2i}, & 1 \leqslant i = j-2 \leqslant N-1 \\ \frac{1}{2i}, & i = j = N \text{ and } i = j = N+1 \\ 0, & \text{otherwise.} \end{cases}$$

We want to eliminate vector a^1 in (29) and replace it with the vector $A^T = [a_0(t), a_1(t), \cdots, a_N(t)]$. Using the expansion (19) (truncated after $N+1$ term) to represent the near-end boundary voltage, $v(-1,t)$, and taking into account that $T_k(-1) = (-1)^k$, we obtain

$$\sum_{k=0}^{N+1}{}' (-1)^k a_k(t) = v(-1,t)$$

or else

$$a_{N+1}(t) = \sum_{k=0}^{N}{}' (-1)^{N+k} a_k(t) - (-1)^N v(-1,t). \quad (30)$$

Using this relation we can now write

$$a^1 = QA + e_N v(-1,t) \quad (31a)$$

here Q is a $(N+1)\times(N+1)$ square matrix and e_N is a $(N+1)$-dimensional vector:

$$e_N^T = \left[0, 0, \cdots, 0, -(-1)^N\right].$$

The matrix Q is defined as follows: (31b), shown above.

The formula (31a) used in (29) yields the desired relation between the vectors A and A^* in the form

$$QA + e_N v(-1,t) = HA^*. \quad (32)$$

The equations (26) written for the series truncated at N, and multiplied from the left by the matrix H, yield

$$QA + e_N v(-1,t) = HK_r B + HK_l \frac{dB}{dt} \quad (33)$$

where K_r, K_l are truncated $(N+1)\times(N+1)$ matrices obtained from infinite matrices $\tilde{K}_r$, $\tilde{K}_l$ and

$$B^T = [b_0(t), b_1(t), \cdots, b_N(t)].$$

The initial conditions $B(0)$ are determined using the line initial current distribution (6):

$$b_k(0) = \begin{cases} 2\langle i(x,0), 1\rangle & k=0; \\ \langle i(x,0), T_k(x)\rangle, & 1 \leqslant k \leqslant N. \end{cases} \quad (34)$$

An analogous procedure is applied to equations (24b) with the difference that in eliminating the coefficients $b_k^*(t)$ for the expansion of current derivatives by the coefficients $b_k(t)$ defining the current expansion, we use the far-end boundary condition, $i(1,t)$, for the current and the fact that $T_k(1) = 1$. The resulting equations are

$$Q_1 B + e_{N1} i(1,t) = HK_g A + HK_c \frac{dA}{dt} \quad (35)$$

where Q_1 is an $(N+1)\times(N+1)$ square matrix, e_{N1} is an $(N+1)$-dimensional vector defined as $e_{N1}^T = [0, 0, \cdots, 0, 1]$, and

$$K_c(i,j) = -\frac{1}{2}(c_{i+j} + c_{|i-j|}), \qquad i,j = 0,1,2,\cdots,N$$

$$K_g(i,j) = -\frac{1}{2}(g_{i+j} + g_{|i-j|}), \qquad i,j = 0,1,2,\cdots,N. \quad (36)$$

The matrix Q_1 has the same structure as the matrix Q defined in (31b) but the last row has as its first entry $-1/2$ and the remaining entries are all of value -1. The initial conditions, $A(0)$, are determined using the initial distribution of voltage in the line as given in (5) and the procedure analogous to the one determined by (34).

IV. Spectral Equations for Multiple Lines

The treatment of multiple-line equations is analogous to the one for a single line. We expand the line voltages and currents in series:

$$v_j = \sum_{k=0}^{\infty}{}' a_k^j(t) T_k(x)$$

$$i_j = \sum_{k=0}^{\infty}{}' b_k^j(t) T_k(x) \quad (37)$$

where $a_k^j(t), b_k^j(t)$, $j = 0,1,2,\cdots,\mathscr{K}$, are unknown coefficients to be computed. Those are arranged in vectors $\boldsymbol{A}, \boldsymbol{B}$ with entries A_j, B_j defined as follows:

$$A_j = [a_0^j(t), a_1^j(t), \cdots]^T$$

$$B_j = [b_0^j(t), b_1^j(t), \cdots]^T. \quad (38)$$

The line parameters (entries of $\boldsymbol{L}(x), \boldsymbol{C}(x), \boldsymbol{R}(x), \boldsymbol{G}(x)$ matrices) are also expanded into Chebyshev series:

$$l_{jn}(x) = \sum_{k=0}^{\infty}{}' l_k^{jn} T_k(x)$$

$$c_{jn}(x) = \sum_{k=0}^{\infty}{}' c_k^{jn} T_k(x)$$

$$r_{jn}(x) = \sum_{k=0}^{\infty}{}' r_k^{jn} T_k(x)$$

$$g_{jn}(x) = \sum_{k=0}^{\infty}{}' l_k^{jn} T_k(x). \quad (39)$$

These expansions are then applied to equations (7) and (8) and the properties of Chebyshev polynomials are used to construct the truncated equations for the vectors A, B of unknown coefficients. The procedures are described in the Appendix. The resulting equations are

$$Q_1 B_j + e_{N1} i_j(1,t) = \sum_{n=1}^{\mathscr{K}} HK_{jn}^g A_n + \sum_{n=1}^{\mathscr{K}} HK_{jn}^c \frac{dA_n}{dt}$$

$$QA_j + e_N v_j(-1,t) = \sum_{n=1}^{\mathscr{K}} HK_{jn}^r B_n + \sum_{n=1}^{\mathscr{K}} HK_{jn}^l \frac{dB_n}{dt} \quad (40)$$

$$j = 1,2,\cdots,\mathscr{K}$$

where H is the matrix defined in (29), Q and Q_1 are the matrices defined in (31b) and (35), respectively, e_N and e_{N1} are the vectors defined in (31a) and (35), respectively, and K_{jn}^l, K_{jn}^c, K_{jn}^r, and K_{jn}^g are square $(N+1)\times(N+1)$ matrices formed (assuming the truncation of Chebyshev series at N) by the known coefficients of line parameter expansions (see the Appendix).

Introducing the $\mathscr{K}(N+1)\times\mathscr{K}(N+1)$ square matrices

$$\tilde{K}_l = H\{K_{ij}^l\}$$

$$\tilde{K}_c = H\{K_{ij}^c\}$$

$$\tilde{K}_r = H\{K_{ij}^c\}$$

$$\tilde{K}_g = H\{K_{ij}^g\}$$

$$i,j = 1,2,\cdots,\mathscr{K}$$

$$\boldsymbol{Q} = \operatorname{diag}\{Q\}$$

$$\boldsymbol{Q}_1 = \operatorname{diag}\{Q_1\}$$

$$\boldsymbol{E} = \operatorname{diag}\{e_N\}$$

$$\boldsymbol{E}_1 = \operatorname{diag}\{e_{N1}\}$$

$$\boldsymbol{v}(-1,t) = [v_1(-1,t), v_2(-1,t), \cdots, v_{\mathscr{K}}(-1,t)]^T$$

$$\boldsymbol{i}(1,t) = [i_1(1,t), i_2(1,t), \cdots, i_{\mathscr{K}}(1,t)]^T \quad (41)$$

we can write (40) in compact form:

$$\boldsymbol{Q}_1\boldsymbol{B} + \boldsymbol{E}_1\boldsymbol{i}(1,t) = \tilde{K}_g\boldsymbol{A} + \tilde{K}_c\frac{d\boldsymbol{A}}{dt}$$

$$\boldsymbol{Q}\boldsymbol{A} + \boldsymbol{E}\boldsymbol{v}(-1,t) = \tilde{K}_r\boldsymbol{B} + \tilde{K}_l\frac{d\boldsymbol{B}}{dt} \quad (42)$$

which is analogous to (33), (35). In the definitions (41) the symbol "diag$\{(\cdot)\}$" designates a block diagonal matrix composed of identical blocks $(\cdot)$. The initial conditions, $\boldsymbol{A}(0)$, $\boldsymbol{B}(0)$ are determined using relations (11) and (12) in a way similar to the one used in the case of a single line.

V. Computational Considerations

Equations (42) describing the evolution of expansion coefficients in the case of multiple lines have the same form as (33) and (35), corresponding to a single-line case. Further discussion will therefore be conducted in relation to (42). This section is devoted to a discussion of numerical treatment of (42), determining the expansion coefficients. Introducing the vector notation

$$P=\begin{pmatrix} A \\ B \end{pmatrix} \tag{43}$$

we can write (42) in the form

$$M_l\frac{dP}{dt}+M_rP=EW \tag{44}$$

where M_l, M_r, and E are $(2M+2)\times(2M+2)$ square matrices with constant entries, and W is the vector of forcing functions $W^T=[v(-1,t), i(1,t)]$. The matrices introduced in (44) are defined as follows:

$$M_l=\begin{pmatrix} \tilde{K}_c & 0 \\ 0 & \tilde{K}_l \end{pmatrix}$$

$$M_r=\begin{pmatrix} \tilde{K}_g & -Q_1 \\ -Q & \tilde{K}_r \end{pmatrix}$$

$$E=\begin{pmatrix} 0 & E_{N1} \\ E_N & 0 \end{pmatrix}.$$

Equation (44) is discretized using the popular backward differentiation formula (BDF) for the derivative approximation:

$$\left.\frac{dP}{dt}\right|_{t=t_n}=\frac{1}{h}\sum_{j=0}^{k}\alpha_jP_{n-j} \tag{45}$$

where h is the integration step size, α_j and k are constants characteristic for a specific type of BDF, and P_i denotes the numerical approximation to the exact solution $P(t_i)$ of the differential equation at a discrete moment of time, t_i. Application of (45) to (44), expressed for the time $t=t_n$, yields

$$\left(\frac{\alpha_0}{h}M_l+M_r\right)P_n=EW_n-\frac{1}{h}M_l\sum_{j=1}^{k}\alpha_jP_{n-j}. \tag{46}$$

In particular for two-step Gear's method [20] ($k=2, \alpha_0=\frac{3}{2}, \alpha_1=-2, \alpha_2=\frac{1}{2}$) we have

$$\left(\frac{3}{2h}M_l+M_r\right)P_n=EW_n+\frac{1}{h}\left(2M_lP_{n-1}-\frac{1}{2}M_lP_{n-2}\right). \tag{47}$$

Computations based on (47) require a additional, single-step formula for starting at $t=0$ and after each change of step size.

An alternative integration formula can be built using the matrix exponential. Equations (44) are premultiplied (from the left) by the inverse of M_l ($\det M_l\neq 0$ because $\tilde{K}_l$ and $\tilde{K}_c$ are not singular), yielding

$$\frac{dP}{dt}=KP+FW \tag{48}$$

where K is a square, $2\mathscr{K}(N+1)\times 2\mathscr{K}(N+1)$, matrix defined as follows:

$$K=\begin{pmatrix} -\tilde{K}_c^{-1}\tilde{K}_g & \tilde{K}_c^{-1}Q \\ \tilde{K}_l^{-1}Q & -\tilde{K}_l^{-1}\tilde{K}_r \end{pmatrix}$$

and F is a rectangular, $2\mathscr{K}(N+1)\times 2\mathscr{K}$, matrix of the form

$$F=\begin{pmatrix} 0 & \tilde{K}_c^{-1}E_{N1} \\ \tilde{K}_l^{-1}E_N & 0 \end{pmatrix}.$$

Using the transition matrix technique [21] we can write (48) in the difference form

$$P(t_n)=GP(t_{n-1})+\Delta P(t_n) \tag{49}$$

where G is the matrix exponential

$$G=e^{K\Delta t} \tag{50}$$

and $\Delta P(t_n)$ is the increment

$$\Delta P(t_n)=\int_0^{\Delta t}e^{K(\Delta t-\tau)}FW(t_{n-1}+\tau)\,d\tau. \tag{51}$$

Equation (49) forms the basis for simple numerical computation of time evolution of vectors $\boldsymbol{A}, \boldsymbol{B}$.

VI. Circuit Model of Transmission Line System

The analysis provided above allows us to derive a model of a transmission line system in the form of an equivalent circuit which is suitable for implementation in a circuit analyzer. Equation (49) can be written in the form

$$P_n=GP_{n-1}+\tilde{C}_1W_n+\tilde{C}_2W_{n-1} \tag{52}$$

where the vector W_n represents voltages at the ends of the lines

$$W_n=\begin{Bmatrix} v(-1,t_n) \\ i(1,t_n) \end{Bmatrix}$$

and P_n represents the numerical approximation to $P(t_n)$. This approximation is obtained by replacing the vector function, $w(t_{n-1}+\tau)$, in the integrand with its linear interpolation based on the end values W_{n-1} and W_n. More sophisticated approximations are available [21], but will not be discussed in this paper. The rectangular $2\mathscr{K}(N+1)\times 2\mathscr{K}$ matrices $\tilde{C}_1$ and $\tilde{C}_2$ are defined as follows:

$$\tilde{C}_1=\frac{1}{\Delta t}\int_0^{\Delta t}\tau e^{K(\Delta t-\tau)}F\,d\tau$$

$$\tilde{C}_2=\int_0^{\Delta t}e^{K(\Delta t-\tau)}F\,d\tau-\tilde{C}_1. \tag{53}$$

Equation (52) can be used to determine the equivalent circuit for the system of multiple coupled lines. To sim-

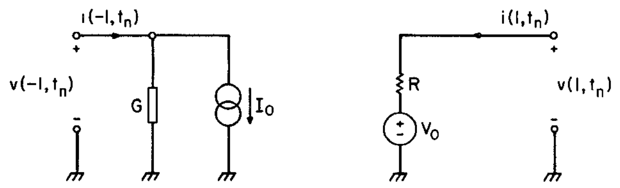

Fig. 1. Equivalent circuit of transmission lines (for the moment $t = t_n$). I_0, V_0 are independent current and voltage sources determined by the solutions at $t = t_{n-1}$.

plify the notation we restrict the discussion to the case of a single line only. The results can be extended to multiple lines without any conceptual difficulty. It will be convenient to introduce the following $2(N+1)$-dimensional vectors:

$$e_1^T = \left(\frac{1}{2}, 1, \cdots, 1, 0, \cdots, 0\right)$$

$$e_2^T = \left(0, \cdots, 0, \frac{1}{2}, -1, 1, \cdots, (-1)^N\right). \quad (54)$$

Using (54), the definition of vector P_n, expansions (19) and (20), and the fact that $T_n(1) = 1$, $T_n(-1) = (-1)^n$, we obtain

$$e_1^T P_n = v(1, t_n)$$

and

$$e_2^T P_n = i(-1, t_n). \quad (55)$$

Multiplication of (52) (from the left) by e_1^T and subsequently by e_2^T yields therefore

$$v(1, t_n) = e_1^T \tilde{C}_2 W_n + e_1^T (G P_{n-1} + \tilde{C}_1 W_{n-1})$$

$$i(-1, t_n) = e_2^T \tilde{C}_2 W_n + e_2^T (G P_{n-1} + \tilde{C}_1 W_{n-1}). \quad (56)$$

The second term on the right side of each of the above equations depends on previously computed quantities and is thus considered to be given in the solution for step n. These terms will be denoted

$$e_1^T (G P_{n-1} + \tilde{C}_1 W_{n-1}) = V_0$$

$$e_2^T (G P_{n-1} + \tilde{C}_1 W_{n-1}) = I_0. \quad (57)$$

Taking into account the structure of matrix F and the definition of the vector $W_n^T = [v(-1, t_n), i(1, t_n)]$, it is easy to verify that

$$e_1^T \tilde{C}_2 W_n = R_{eq} i(1, t_n)$$

$$e_2^T \tilde{C}_2 W_n = G_{eq} v(-1, t_n)$$

where R_{eq} and G_q are constants which we call the equivalent resistance and the equivalent conductance.

Using these results and the definitions (57) in (56), we obtain the following form of difference equations (52) of the transmission line:

$$v(1, t_n) = R_{eq} i(1, t_n) + V_0$$

$$i(-1, t_n) = G_{eq} v(-1, t_n) + I_0. \quad (58)$$

This form defines the equivalent circuit shown in Fig. 1.

TABLE I
COMPARISON OF CPU TIME (VAX-11/750 VMS) IN COMPUTING USING DIFFERENT METHODS

Example	SPECTRAL	UACSL*	SPICE
1	20 sec.	8 sec.	≥ 100 sec
2	14 sec.	12–14 sec.	≥ 150 sec.
3	20 sec.	not applicable	not computed
4	360 sec.	370 sec.***	not computed**
5	199 sec.	not applicable	4 hrs 6 min

*Results obtained using the program UACSL [22], based on time-domain modal analysis.
**Estimated CPU time will be several hours.
***Running simplified line model (assuming zero losses) with the use of expanded UACSL, which allows simulation of nonlinear terminations.

VII. NUMERICAL EXAMPLES

To illustrate the properties of the algorithm discussed in this paper, some specific examples are presented. The numerical results were compared either with published experimental results (if available [1]) or with computations performed using other programs based on time-domain modal analysis [22] and the SPICE simulation. The results of comparisons are very encouraging; the CPU times listed in Table I show that the efficiency of this method is indeed impressive.

Example 1: A Three-Conductor Lossless Microstrip

The dimensions of the microstrips and their external circuit terminations for this example are taken from [1]. The capacitance (in pF/cm) and inductance (in nH/cm) matrices of the microstrips are, respectively,

$$C = \begin{pmatrix} 1.0413 & -0.3432 & -0.0140 \\ -0.3432 & 1.1987 & -0.3432 \\ -0.0140 & -0.3432 & 1.0413 \end{pmatrix}$$

$$L = \begin{pmatrix} 3.8790 & 1.6238 & 0.8285 \\ 1.6238 & 3.7129 & 1.6238 \\ 0.8285 & 1.6238 & 3.8790 \end{pmatrix}$$

The input voltage source (in V) is

$$e(t) = \begin{cases} 10t, & t \leqslant 0.1 \text{ ns} \\ 1.0 & t \geqslant 0.1 \text{ ns}. \end{cases}$$

The waveforms of the transient responses computed using our program are presented in Fig. 2. They are close to the experimental ones given in [1] within recording accuracy of about 5 percent. The corresponding CPU time is listed in the Table I.

Example 2: Two-Conductor Lossless Lines with Dynamic Circuit Terminations

The tested circuit is shown in Fig. 3; the line length $s = 2.8$ cm. The parameters of the two lines are:

$$1 = 0.0656 \text{ nH/m}$$

$$c = 0.98 \text{ pF/m}$$

$$l_m = 0.0128 \text{ nH/m}$$

$$c_m = -0.117 \text{ pF/m}$$

where l and l_m are self and mutual inductances and c and c_m are self and mutual capacitances. The input voltage

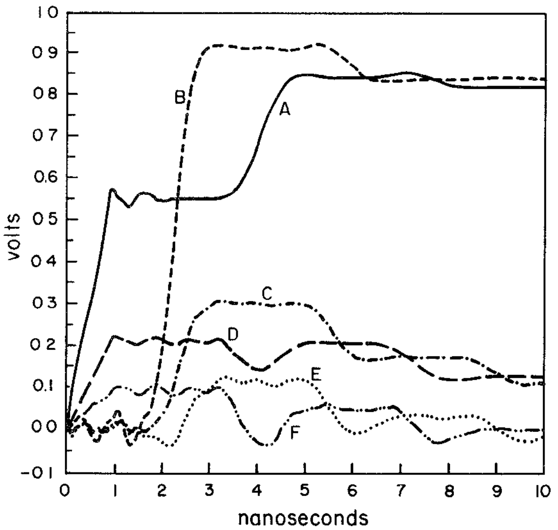

Fig. 2. Transient response of the three-conductor system. A—near-end voltage on active line (V_{1a}). B—Far-end voltage on active line (V_{1b}). C,D,E,F—Crosstalk voltages (V_{2b}), (V_{2a}), (V_{3b}), (V_{3a}), respectively, on the lines 2 and 3. Note: The symbols in parenthesis are the same as those in [reference 1, figs. 8 and 9].

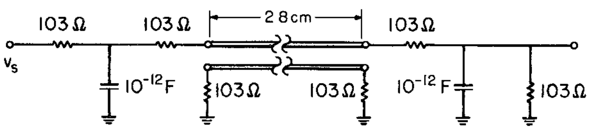

Fig. 3. Two-conductor transmission line with linear terminating networks.

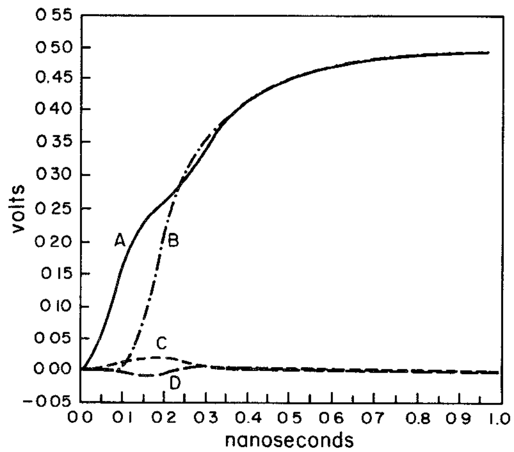

Fig. 4. Transient voltages in the two-conductor transmission line systems given in Fig. 3. A—Near-end on active line. B—Far-end on active line. C—Near-end on quiescent line. D—Far-end on quiescent line.

source (in V) is

$$v_s(t) = \begin{cases} 10t, & t \leqslant 0.1 \text{ ns} \\ 1 & t \geqslant 0.1 \text{ ns}. \end{cases}$$

The computed waveforms of transient responses are given in Fig. 4. The waveforms were compared to those computed using the UACSL program [22] and SPICE (model in the form of a chain of L, C lumped circuits). The solutions were very close within 1 percent accuracy. The CPU time necessary for solution is shown in the Table I.

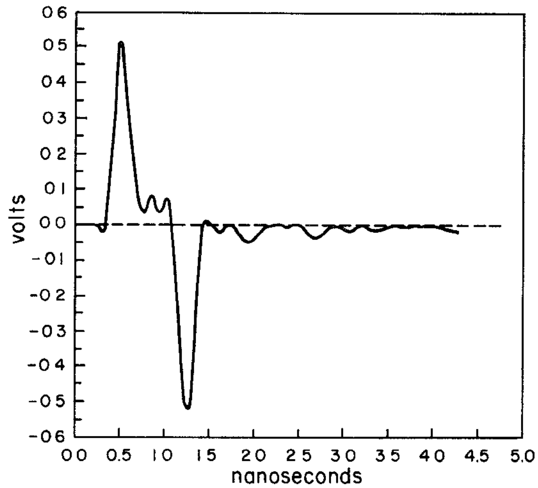

Fig. 5. Crosstalk voltage in the middle of a quiescent line, computed using the spectral technique.

Example 3: Two-Identical-Conductor Lossy Nonuniform Lines

The example transmission system is described in [9]. The parameters of the two lines having the same length of $s = 2$ cm are

$$l = \frac{l_0}{1+k(x)}$$

$$l_m = k(x) * l(x)$$

$$c = \frac{c_0}{1-k(x)}$$

$$c_m = k(x) * c(x)$$

$$k(x) = 0.25\left(1 + 0.6\sin\left(\pi x + \frac{\pi}{4}\right)\right)$$

$$l_0 = 3.87 \text{ pH/m}$$

$$c_0 = 1.0413 \text{ pF/m}$$

$$r = 1.2\ \Omega/\text{m}$$

$$r_m = 0.$$

$$g = g_m = 0.$$

The symbols l, l_m, c, and c_m have the same meanings as in Example 2. The input voltage source (in V) is

$$v_s(t) = \begin{cases} 2t, & t \leqslant 0.5 \text{ ns} \\ 1, & 0.5 \text{ ns} \leqslant t \leqslant 1 \text{ ns} \\ 1-2(t-1), & 1 \text{ ns} \leqslant t \leqslant 1.5 \text{ ns} \\ 0 & t \geqslant 1.5 \text{ ns}. \end{cases}$$

The model of this transmission system was implemented using our prototype program based on the spectral technique. The transients were computed, and the results compared favorably to those given in [9]. The corresponding CPU time is given in Table I. An example of cross talk voltage in the middle of quiescent line (line 2 in [9]) computed using our program is shown in Fig. 5. The result corresponds to [9, fig. 14].

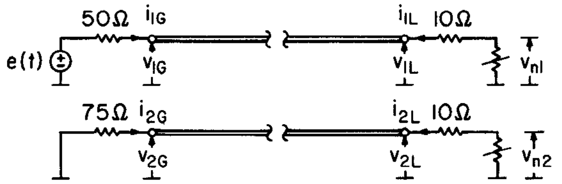

Fig. 6. Two-conductor transmission line with nonlinear terminations.

Example 4: Two-Conductor Lossy Transmission Lines with Nonlinear Terminations

The algorithm based on spectral techniques can be easily used to compute the transients in the lines with nonlinear terminations. To illustrate this capability, we use two conductor lines, considered in [7], having a length of 50 cm and terminated as shown in Fig. 6. The parameters of lines (assuming here to be frequency independent) are

$$l = 309 \text{ nH/m}$$
$$l_m = 21.7 \text{ nH/m}$$
$$c = 144 \text{ pF/m}$$
$$c_m = -6.4 \text{ pF/m}$$
$$r = 524 \text{ m}\Omega/\text{m}$$
$$r_m = 33.9 \text{ m}\Omega/\text{m}$$
$$g = 905 \text{ nS/m}$$
$$g_m = -11.8 \text{ nS/m}.$$

The nonlinear "resistances" are characterized by the relation

$$I = 10(e^{40V} - 1)$$

where I is the current in nA flowing through the "resistor" and v is the corresponding voltage drop in V. The input voltage source is shown in Fig. 7(a). The transient voltages were computed and CPU time recorded in Table I. The results for active line are plotted in Fig. 7(b).

Example 5: Prototype Interconnections in a Chip Carrier

Interconnections in chip carriers are usually nonuniform because of the space constraints in the proximity of the chip. A prototypical two-conductor interconnection is illustrated in Fig. 8(a) and (b). The line and terminating network configuration is shown in Fig. 8(c). The line parameters computed section by section using the technique for parallel uniform lines [11] are given in Table II. The transient caused by the input voltage, $v_s(t)$, shown in Fig. 8(c), was computed using $N = 8$ terms in Chebyshev series. The near-end and far-end voltages on active line are shown in Fig. 9(a). The effects of varying line impedance (changing from low to high) are clearly visible. The corresponding responses on quiescent line are shown in Fig. 9(b). For comparison purposes the nonuniform lines were replaced by two lines of the constant width of 21.4 mils. Remaining parameters (thickness, separation between the axes, distance from the ground plane) were unchanged. The transients (caused by the same input voltage) on active line are shown in Fig. 10. The same results, differing by no more than 1 mV, were obtained using SPICE. Each line was modeled using a chain of 500 L, C elements. The CPU

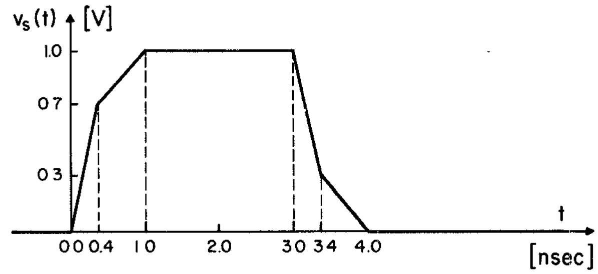

(a)

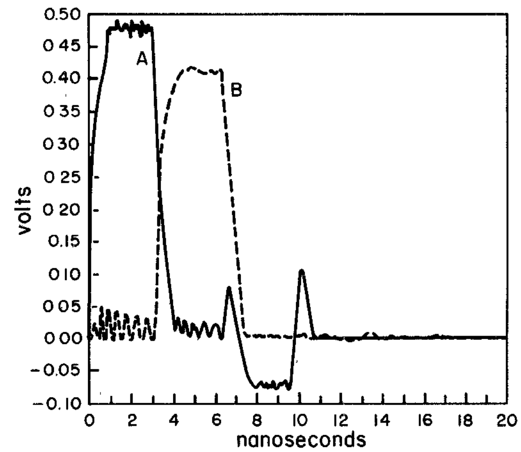

(b)

Fig. 7. Transients in the transmission system with nonlinear terminations. (a) Input voltage, $v_s(t)$. (b) Voltages on the active line: A—Near end, and B—Far end.

time for computing using our program and SPICE is given in Table I. Our program is more than one order magnitude faster than SPICE in this particular application. The CPU time savings will be even greater in applications to systems with more than two conductors.

VIII. Conclusions and Further Research

The spectral technique is used to transform partial differential equations describing a system of transmission lines into a set of linear ordinary differential equations, which can be solved with one of the many well-developed integration techniques. The derivation is somewhat tedious but the resulting evolution equations are very simple and can be solved very efficiently with the help of a digital computer. The numerical experiments performed with the prototype program showed that the method can solve specific problems (lossless, uniform lines) just as fast as less general methods based on modal analysis exploiting the particular properties of lines. This is achieved in spite of the fact that the prototype program utilizes a rather primitive integration method based on the state transition matrix. An obvious improvement that soon will be exploited is better approximation of the integrand in the increment equation. We shall use linear and parabolic interpolation in performing the integration.

In future work, other integration methods will be used in a quest for further efficiency improvements.

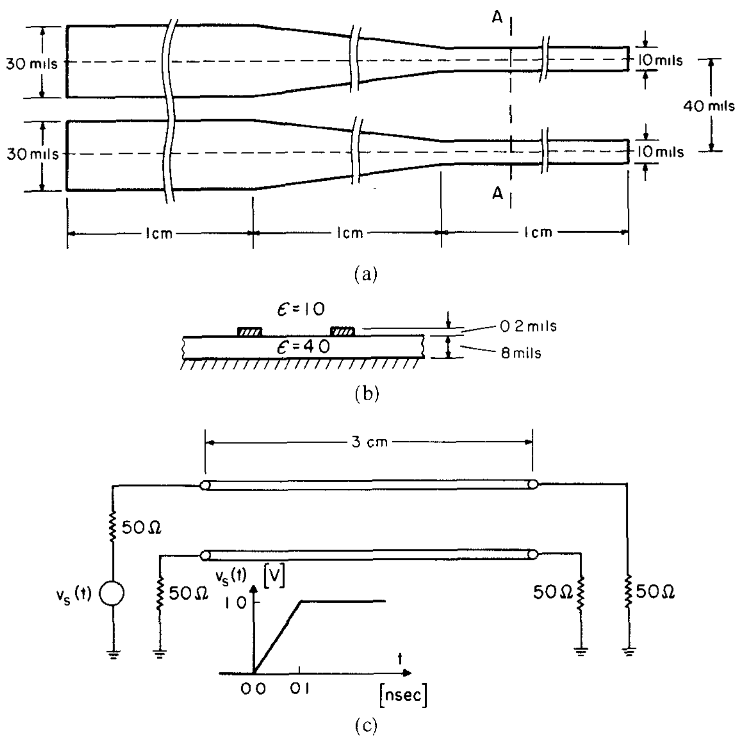

Fig. 8. Fragment of the prototypical interconnection in a chip carrier. (a) Top view of metallization. (b) Geometry of cross-section. (c) Circuit configuration of the interconnection and driving voltage, $v_s(t)$.

TABLE II
PARAMETERS OF NONUNIFORM TRANSMISSION LINE SYSTEM

x cm	$C_{11}=C_{22}$ pF/cm	$C_{12}=C_{21}$ pF/cm	$L_{11}=L_{22}$ nH/cm	$L_{21}=L_{12}$ nH/cm
0.0–1.0	1.84	–0.090	1.96	0.23
1.14	1.76	–0.073	2.04	0.22
1.29	1.60	–0.050	2.22	0.20
1.43	1.44	–0.035	2.43	0.19
1.57	1.28	–0.024	2.69	0.17
1.71	1.12	–0.017	3.01	0.17
1.86	0.96	–0.012	3.44	0.16
2.0–3.0	0.88	–0.009	3.71	0.16

The most important feature of the method is its generality: it can easily be applied to uniform and nonuniform lines. The final algorithm can be used to develop a line equivalent circuit which is helpful in situations where boundary conditions are determined by the networks of passive and active elements (transistors). In such situations the line analysis must be combined with the network analysis, and the use of the equivalent circuit is essential. The version of the algorithm presented in this paper is directly applicable to the analysis of lines with frequency-independent parameters. In some cases, interconnections are modeled more accurately by the lines with frequency-dependent parameters. For such situations further developments of spectral analysis are necessary and will be reported in a separate paper.

APPENDIX
DERIVATION OF SPECTRAL EQUATIONS FOR A SYSTEM OF COUPLED TRANSMISSION LINES

The formulation of spectral equations for multiple transmission lines follows the procedure described for the case of a single line. Thus the expansions defined by (37) and (39) and the expansions for the derivatives

$$\frac{\partial v_j}{\partial x} = \sum_{k=0}^{\infty}{}' a_k^{*}(t) T_k(x)$$

$$\frac{\partial i_j}{\partial x} = \sum_{k=0}^{\infty}{}' b_k^{*}(t) T_k(x) \tag{A1}$$

are used to eliminate the variables representing the line voltages and currents from (7) and (8). The procedures for (7) and (8) are analogous and the discussion given here will be limited to the procedure involving (7) only. The equations are multiplied by Chebyshev polynomials and appropriate inner products are formed. Using previously established properties of Chebyshev polynomials we obtain (after some manipulation) the following equations:

$$\hat{A}_j^{*} = \sum_{n=1}^{\mathscr{K}} K_{jn}^{*r} \hat{B}_n^{*} + \sum_{n=1}^{\mathscr{K}} K_{jn}^{*l} \frac{d\hat{B}_n^{*}}{dt}, \qquad j = 1, 2, \cdots, \mathscr{K} \tag{A2}$$

where $A_j^{*} = (a_0^{*j}(t) \quad a_1^{*j}(t) \quad \cdots)^T$ and $\hat{B}_n^{*}$ are infinite vectors.

The entries of matrices K_{jn}^{*r} and K_{jn}^{*l} are defined as follows:

$$K_{jn}^{*r}(k,m) = \frac{-1}{2}\left(r_{k+m}^{jn} + r_{|k-m|}^{jn}\right)$$

$$K_{jn}^{*l}(k,m) = \frac{-1}{2}\left(l_{k+m}^{jn} + l_{|k-m|}^{jn}\right), \qquad k, m = 1, 2, \cdots. \tag{A3}$$

The matrices K_{jn}^{*r} and K_{jn}^{*l} are infinite. In practical

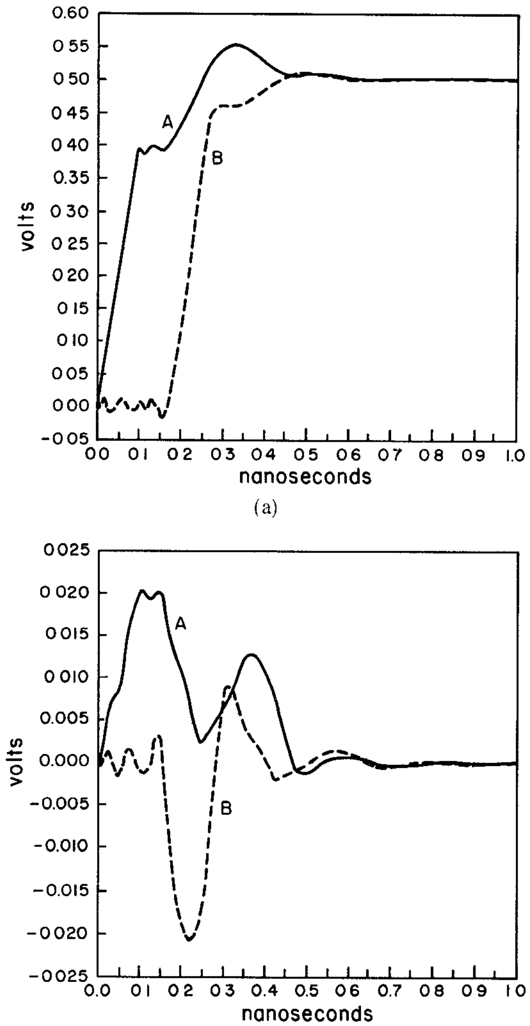

(a)

(b)

Fig. 9. Transients in the nonuniform interconnection. (a) Voltages on the active line: A—Near-end, and B—Far end. (b) Voltages on the quiescent line: A—Near-end, and B—Far end.

computations we use Chebyshev series which are truncated at N, and therefore those matrices are also truncated. The resulting truncated matrices, denoted K_{jn}^{r}, K_{jn}^{l}, are square and have dimensions of $(N+1)\times(N+1)$. We then use relations of the type given by (27) and (28) between the coefficients of expansions for the functions and their derivatives, which with truncation of series at $k=N$ can be written is the form

$$\begin{pmatrix} a_1^j(t) \\ a_2^j(t) \\ \vdots \\ a_{N+1}^j(t) \end{pmatrix} = HA_j^* \tag{A4}$$

where H is the conversion matrix defined in (29) and A_j^* is a truncated vector of expansion coefficients for the derivatives

$$A_j^* = \left(a_0^{*j}(t) \quad a_1^{*j}(t) \cdots a_N^{*j}(t)\right)^T.$$

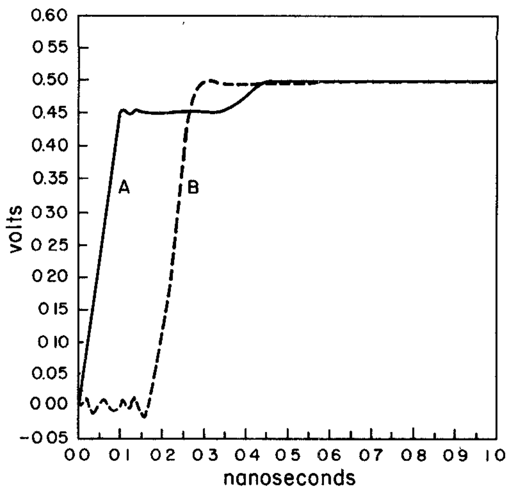

Fig. 10. Transient voltages on the active line of uniform transmission system. A—Near-end. B—Far-end.

Using near-end voltages $v_j(-1,t)$, we can write

$$(-1)^{N+1}a_{N+1}^j(t) + \sum_{k=0}^{K}{}' (-1)^k a_k^j(t) = v_j(-1,t). \tag{A5}$$

This relation, used in the procedure developed for single-line equation (see (31),(32)), allows us to write (A4) in the form

$$QA_j + e_N v_j(-1,t) = HA_j^* \tag{A6}$$

where Q is the matrix defined in (31b) and e_N is the vector defined in (31a). Using (A6) in (A2), with truncation of series after the Nth term, we obtain (40b). Equations (40a) are obtained following an analogous procedure with the use of far-end currents, $i_j(1,t)$, in building the relation

$$Q_1 B_j + e_{N1} i_j(1,t) = HB_j^*$$

between the truncated vectors of coefficients for current, B_j, and current derivatives, B_j^*, respectively. The matrix Q_1 and the vector e_{N1} are the same as those used in developing (35). The truncated matrices K_{jn}^{g} and K_{jn}^{c} have entries defined as follows:

$$K_{jn}^{c}(k,m) = \frac{-1}{2}\left(c_{k+m}^{jn} + c_{|k-m|}^{jn}\right)$$
$$K_{jn}^{g}(k,m) = \frac{-1}{2}\left(g_{k+m}^{jn} + g_{|k-m|}^{jn}\right), \qquad k,m = 1,2,\cdots,N. \tag{A7}$$

Acknowledgment

The authors would like to express their gratitude to the students participating in the research seminars for their discussions and for assistance in conducting this work. In particular, they would like to thank J. C. Liao and M. W. Guarini for sharing the results of their research.

References

[1] F. Y. Chang, "Transient analysis of lossless coupled transmission lines in a nonhomogeneous dielectric medium," *IEEE Trans. Microwave Theory Tech.*, vol. MTT-18, pp. 616–626, Sept. 1970.

[2] V. Dvorak, "Computer simulation of signal propagation through a nonuniform transmission line," *IEEE Trans. Circuit Theory*, vol. CT-20, pp. 580–583, Sept. 1973.

[3] J. E. Adair and G. I. Haddad, "Coupled-mode analysis of nonuniform coupled transmission lines," *IEEE Trans. Microwave Theory Tech.*, vol. MTT-17, pp. 746–752, Oct. 1969.
[4] G. M. L. Gladwell and S. Coen, "A Chebyshev approximation method for microstrip problem," *IEEE Trans. Microwave Theory Tech.*, vol. MTT-23, pp. 865–870, Nov. 1975.
[5] Q. Gu and J. A. Kong, "Transient analysis of single and coupled lines with capacitively loaded junctions," *IEEE Trans. Microwave Theory Tech.*, vol. MTT-34, pp. 952–964, Sept. 1986.
[6] A. R. Djordjevic, T. K. Sarkar, and R. F. Harrington, "Time-domain response of multiconductor transmission lines," *Proc. IEEE*, pp. 743–764, June 1987.
[7] A. R. Djordjevic, T. K. Sarkar, and R. F. Harrington, "Analysis of lossy transmission lines with arbitrary nonlinear terminal networks," *IEEE Trans. Microwave Theory Tech.*, vol. MTT-34, pp. 660–666, June 1986.
[8] C. S. Chang, "Transmission lines," in *Advances in CAD for VLSI*, vol. 3, pt. 2, A. Ruehli, Ed. Amsterdam: Elsevier, 1987, sec. 11.3, pp. 292–332.
[9] Y. C. Yang, J. A. Kong, and Q. Gu, "Time-domain perturbational analysis of nonuniform coupled transmission lines," *IEEE Trans. Microwave Theory Tech.*, vol. MTT-33, pp. 1120–1130, Nov. 1985.
[10] C. Wei, R. F. Harrington, J. R. Mautz, and T. K. Sarkar, "Multiconductor, transmission lines in multiplayered dielectric media," *IEEE Trans. Microwave Theory Tech.*, vol. MTT-32, pp. 439–450, Apr. 1984.
[11] M. R. Scheinfein and O. A. Palusinski, "Calculation of electrical parameters for electronic packaging applications," *Trans. Soc. Comput. Simulation*, vol. 4, no. 3, pp. 186–254, July 1987.
[12] A. C. Cangellaris, J. L. Prince, and O. A. Palusinski, "Modeling of high-speed interconnects: An integral equation approach to inductance computation," in *Proc. 1988 Summer Comp. Simul. Conf.* (Seattle, WA), July 25–28, 1988.
[13] D. Gottlieb and S. A. Orszag, *Numerical Analysis of Spectral Methods: Theory and Applications*. Philadelphia, PA: SIAM, 1977.
[14] L. Lustman, "The time evolution of spectral discretizations of hyperbolic systems," *SIAM J. Numer. Anal.*, vol. 23, pp. 1193–1198, 1986.
[15] Robert G. Voigt, David Gottlieb, and M. Yousuff Hussaini, "Spectral Method for Partial Differential Equations. *Philadelphia, PA: SIAM*, 1984.
[16] G. Dahlquist, A. Bjorck, *Numerical Methods*. Englewood Cliff, NJ: Prentice Hall, 1984.
[17] B. Gustafsson, H. O. Kreiss, and A. Sundstrom, "Stability theory of difference approximation for mixed initial boundary value problem. II," *Math. Comput.*, vol. 26, pp. 649–686, 1972.
[18] L. N. Treethen and M. R. Trummer, "An instability phenomenon in spectral methods," *SIAM J. Numer. Anal.*, vol. 24, no. 2, pp. 1008–1023, Oct. 1987.
[19] O. A. Palusinski, M. W. Guarini, and S. J. Wright, "Spectral technique in electronic circuit analysis," *Int. J. Numer. Modelling, Electronic Networks, Devices and Fields*, 1988; also O. A. Palusinski, M. W. Guarini, and A. Lee, "Efficient method for simulation MOS integrated circuits," Final Rept. for SRC under Contract 83-01-038, Tucson, July, 1987.
[20] C. W. Gear, *Numerical Initial Value Problems in Ordinary Differential Equations*. Englewood Cliffs, NJ: Prentice-Hall, 1971.
[21] O. A. Palusinski and J. V. Wait, "Simulation methods for combined linear and nonlinear systems," *Simulation*, vol. 30, no. 3, pp. 85–94, Mar. 1978.
[22] J. C. Liao, O. A. Palusinski, and J. L. Prince, "Simulation of electrical performance of board level interconnections," in *Proc. 1987 IEPS Conf.* (Boston), Nov. 8–11, 1987, pp. 923–931.

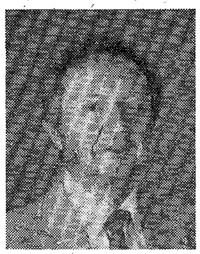

Olgierd A. Palusinski (SM'79) received his M.S. and Ph.D. degrees in electrical engineering at the Technical University in Gliwice, Poland, and the Docteur de l'Université degree at the University of Lille, Lille, France.

He is an Associate Professor of Electrical and Computer Engineering at the University of Arizona in Tucson. His primary research interests are in the areas of simulation techniques for large dynamic systems and their applications in the fields of VLSI circuit and packaging design and analysis.

Anyu Lee was born in Zhangqin, China, on October 7, 1963. He received the B.S. and M.S. degrees in computational fluid mechanics in 1982 and 1985, respectively, from Shanghai Jiao Tong University, Shanghai, P.R. China. In 1988 he was awarded the M.S. degree in electrical engineering from the University of Arizona, Tuscon.

His primary research interests are in the areas of integrated circuit and transmission line simulation.